Brain Struct Funct (2016) 221:879–890
DOI 10.1007/s00429-014-0942-2

ORIGINAL ARTICLE

Predictive coding for motion stimuli in human early visual cortex

Wouter Schellekens · Richard J. A. van Wezel · Natalia Petridou · Nick F. Ramsey · Mathijs Raemaekers

Received: 14 May 2014 / Accepted: 7 November 2014 / Published online: 2 December 2014

Abstract The current study investigates if early visual cortical areas, V1, V2 and V3, use predictive coding to process motion information. Previous studies have reported biased visual motion responses at locations where novel visual information was presented (i.e., the motion trailing edge), which is plausibly linked to the predictability of visual input. Using high-field functional magnetic resonance imaging (fMRI), we measured brain activation during predictable versus unpreceded motion-induced contrast changes during several motion stimuli. We found that unpreceded moving dots appearing at the trailing edge gave rise to enhanced BOLD responses, whereas predictable moving dots at the leading edge resulted in suppressed BOLD responses. Furthermore, we excluded biases in directional sensitivity, shifts in cortical stimulus representation, visuo-spatial attention and classical receptive field effects as viable alternative explanations. The results clearly indicate the presence of predictive coding mechanisms in early visual cortex for visual motion processing, underlying the construction of stable percepts out of highly dynamic visual input.

Keywords High-field fMRI · Motion suppression · Predictive coding · Visual cortex · Visual motion

W. Schellekens (✉) · N. F. Ramsey · M. Raemaekers
Brain Center Rudolf Magnus, UMC Utrecht, Str. 4.205, Postbus 85060, 3508 AB Utrecht, The Netherlands
e-mail: w.schellekens@umcutrecht.nl

R. J. A. van Wezel
Department of Biophysics, Donders Institute for Brain, Cognition and Behaviour, Radboud University Nijmegen, Nijmegen, The Netherlands

R. J. A. van Wezel
Biomedical Signals and Systems, MIRA, University of Twente, Enschede, The Netherlands

N. Petridou
Image Sciences Institute/Radiology, UMC Utrecht, Utrecht, The Netherlands

Introduction

The world around us is constantly changing. Objects within our visual field are moving all the time either because of the objects' characteristics or because we are moving ourselves. Nonetheless, we are able to construct stable and coherent percepts from the ever-changing scenery. It is, however, still unclear how stable percepts are formed from such dynamic visual input. Particularly, neural responses to motion pose the following problem: how do neurons in the visual cortex determine, whether detected contrast changes are caused by stimuli moving from receptive fields of neighboring detectors into the neuron's own receptive field, rather than by an unpreceded contrast change?

One currently popular theory, predictive coding, offers an interesting solution to this problem by means of integrating prior information in the form of predictions (Rao and Ballard 1999; Friston 2005). The mismatch between the anticipated and observed input, the prediction error, is used to encode novel information present in the input and alter predictions to better process future sensory input (Wacongne et al. 2012). Neural firing is thought to mainly represent the prediction error (Egner et al. 2010), which represents the predictability of any given input. Thus, predictive coding allows neural activity to be guided by prior information on, for instance, moving objects. In turn, this allows for discriminating between predictable contrast changes that have been detected by other neurons and unpreceded contrast changes.

Although predictive coding offers a viable solution to the aforementioned problem, it is unclear to what extent predictive coding is utilized in visual motion processing. Incoherent motion has been reported to generate enhanced responses compared to coherent motion (McKeefry et al. 1997), which possibly reflects the difference in prediction error. Other imaging studies may also have shown evidence for a motion-related predictive coding mechanism in early visual cortex (Raemaekers et al. 2009; Schellekens et al. 2013). These studies reported visual field-dependent directional motion biases relative to the fovea (radial versus tangential) during perception of moving random dot stimuli. However, these results can also be explained by a more general principle, where BOLD responses are relatively increased at the trailing compared to the leading edge of a motion stimulus. Such principle is plausibly linked to predictive coding, since randomly positioned dots cannot be predicted at the point of appearance within the stimulus, i.e., the trailing edge, as opposed to other parts of a motion stimulus.

In the current study, we investigate whether there is evidence for predictive coding in early visual cortical areas using moving random dot stimuli and functional MRI (fMRI). We hypothesize that in V1, V2, and V3 larger BOLD signals will be measured at the trailing edge of a motion stimulus, where contrast changes are unpreceded and cannot be predicted, compared to the leading edge of the motion stimulus, where contrast changes can be predicted based on visual information detected earlier along the path of motion. Moreover, we hypothesize that the novelty of a motion stimulus offers a more general and simpler explanation for previously observed directional motion biases, than differences in sensitivity for radial versus tangential motion directions. Finally, a control experiment was conducted to exclude spatial attention and classical receptive field effects as alternative explanations to increased BOLD responses at the trailing edge.

Methods

Subjects

Twenty-five healthy volunteers were recruited from the Utrecht University. Sixteen subjects performed the main experiment and nine subjects performed the control experiment. The protocol was approved by the local ethics committee of the University Medical Center Utrecht, in accordance with the Declaration of Helsinki (2013).

Scan protocol

Scanning was performed on a 7 Tesla Philips Achieva scanner (Philips Healthcare, Best, Netherlands) with a 32-channel receive headcoil (Nova Medical, MA, USA). Functional MRI (fMRI) measurements were obtained using an EPI sequence with the following parameters: SENSE factor = 2.2, TR = 1,500 ms, TE = 25 ms, flip angle = 80°, coronal orientation, FOV (AP, FH, LR) = 52 × 190 × 190 mm^3. The acquired matrix had the following dimensions: 26 × 96 × 96, voxel size: 2 × 1.979 × 1.979 mm^3. The functional images were acquired from the posterior 52 mm of the brain, covering the occipital lobe, and slices were angulated along the z-axis so that their orientation was orthogonal relative to the calcarine sulcus. Additionally, a T1-weighted image of the whole brain (1.00 × 0.98 × 0.98 mm^3, FOV = 252 × 200 × 190) and a proton density image of equal dimensions were acquired at the end of the functional sessions.

Stimuli

For stimulus presentation, a desktop PC, a projector and a rear projection screen were used. The stimuli were programmed using C++ software (Stroustrup, 1983, Bell Laboratories, USA). The presentation of the stimuli was triggered by the scanner. All stimuli were projected on a gray background and the mean luminance was held constant at 42.2 cd/m^2. During the presentation of all stimuli, a red fixation dot with a radius of 0.08° visual angle was projected on the center of the screen.

Polar angle mapping

To obtain the boundaries of the separate visual areas V1, V2, and V3, a polar angle mapping stimulus was used. The polar angle mapping stimulus was a rotating wedge of 48° circular angle, with a maximum eccentricity of 15° visual angle along the horizontal axis. The wedge consisted of a checkerboard pattern that switched contrast every 125 ms (8 Hz). The wedge made six full rotations: three times clockwise and three times counterclockwise. A total of 220 volumes were acquired during the polar angle mapping.

Main experiment

Prior to the motion experiments, a custom-designed motion area mapping stimulus was presented. The purpose of this stimulus was to obtain the retinotopic representations of five areas in each hemifield (ten in total), where motion was to be presented during the main motion experiments (Fig. 1). Our target motion areas were two 4.0° × 4.0° areas that were centered at 7.0° eccentricity along the left and right horizontal meridian. The other eight motion areas were located adjacent to the target areas: directly to the right, left, top and bottom. The adjacent areas were all squares with the exact same dimensions as the target area

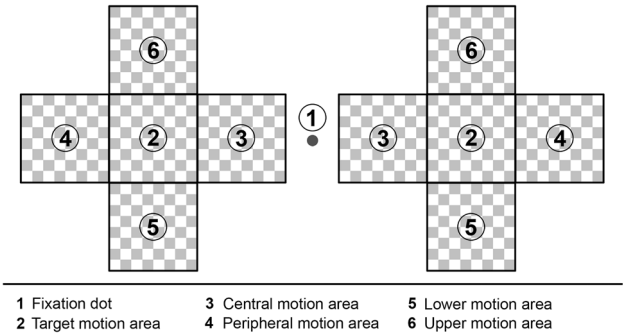

Fig. 1 Main experiment motion areas. Schematic representation of the motion areas. Participants were instructed to maintain focus at the dot at central fixation (*1*) at all times. Each motion area was 4 × 4 visual angle. BOLD responses were obtained only from the target motion area (*2*) that was centered on the horizontal meridian at 7° visual angle

(Fig. 1). All areas were mapped one at a time with a contrast switching checkerboard pattern (8 Hz), which was repeated four times. In total, 240 volumes were acquired during the motion area mapping experiment.

The motion stimuli of the main experiment consisted of moving random dot patterns that were designed to test the effect of predictable motion input at a motion stimuli's leading edge versus unpredictable motion input at a motion stimuli's trailing edge on the amplitude of the BOLD signal. This was achieved by varying the locations of trailing and leading edges of motion stimuli across the previously mapped motion areas, while we measured the BOLD responses in the target motion areas. Only BOLD responses from the target motion areas were used, so that the influence of trailing and leading edges of the motion stimuli was always measured in the exact same retinotopic area. Two motion stimuli were used, one with radial motion and one with tangential motion. Due to time limits that subjects were allowed to be in the scanner, each subject was only presented one of the two motion stimuli, meaning that each motion stimulus was presented to eight subjects.

For the radial motion experiment, dots were projected within the six previously mapped motion areas on the horizontal meridian (three per hemifield), namely the peripheral, target, and central motion areas (Fig. 1). Per motion area, approximately 250 black and white dots were projected (width and height: 0.4° visual angle), moving at a speed of 4.5°/s. We used three categories of stimulus conditions, which varied the distance of leading and trailing edges relative to the target motion area. Category 1: moving dots were presented over the target motion area and 1 adjacent motion area (Fig. 2a, b). In these conditions, either the leading or trailing edge bordered the target motion area, depending on motion areas and direction. Category 2: moving dots were presented over the target motion area only (Fig. 2c). During this condition, both the leading and trailing edge bordered the target motion area, regardless of motion direction. Category 3: moving dots were only presented over 1 motion area adjacent to the target motion area (Fig. 2d, e). Therefore, either the leading or trailing edge bordered the target motion area, while motion was not directly present over the target motion area. The motion direction was either centrifugal or centripetal, and every condition was presented in both hemifields simultaneously. Static dots were presented in the remaining location(s) to keep visual stimulation similar among all conditions. Every motion period lasted for 15 s and was alternated with a 15 s rest period, when all dots were static. All conditions were repeated 3 times and a total of 600 volumes were acquired.

The tangential motion stimulus was similar to the radial motion stimulus, except that dots were now positioned over the target, upper, and lower areas (Fig. 1). The motion direction also changed to upward or downward. However, the same stimulus categories applied: motion over the target motion area and 1 adjacent motion area (Fig. 2f, g); motion over the target motion area only (Fig. 2h); motion over 1 motion area adjacent to the target motion area only (Fig. 2i, j).

Control experiment

The control experiment was conducted on nine participants to investigate confounding factors as classical receptive field (RF) effects and visuo-spatial attention. A classical receptive field representing the trailing edge will detect novel dots directly in its center, rather than in the periphery. As a result, the sequence of a RF's surround and center stimulation may differ greatly at the trailing edge compared to all other parts of a motion stimulus. Possibly, this could lead to relatively enhanced (transient) responses near the trailing edge. Therefore, in contrast to the main experiment, BOLD responses were not obtained from 1 motion area, but from 20 equally spaced locations across the entire width of the screen. This stimulus allowed us to investigate the spatial range of signal enhancements near the trailing edge. The area from which BOLD responses were obtained, the main area, was centered in each hemifield on the horizontal meridian at 8° visual angle, with a width and height of 14° × 4° visual angle (Fig. 3). The cortical representations of the main area's 20 locations were assessed using another custom-designed mapping stimulus, which was a checkerboard pattern (width × height: 3° × 4°; switching contrast: 8 Hz), that moved along the 20 locations in 30 s, and was repeated 8 times (220 volumes in total). After the mapping experiment, approximately 800 square dots (width and height: 0.4°) were randomly projected across the main area. The dots moved (velocity: 4.5°/s) in either a centrifugal or centripetal motion direction for 15 s, alternated with a 15 s stationary period.

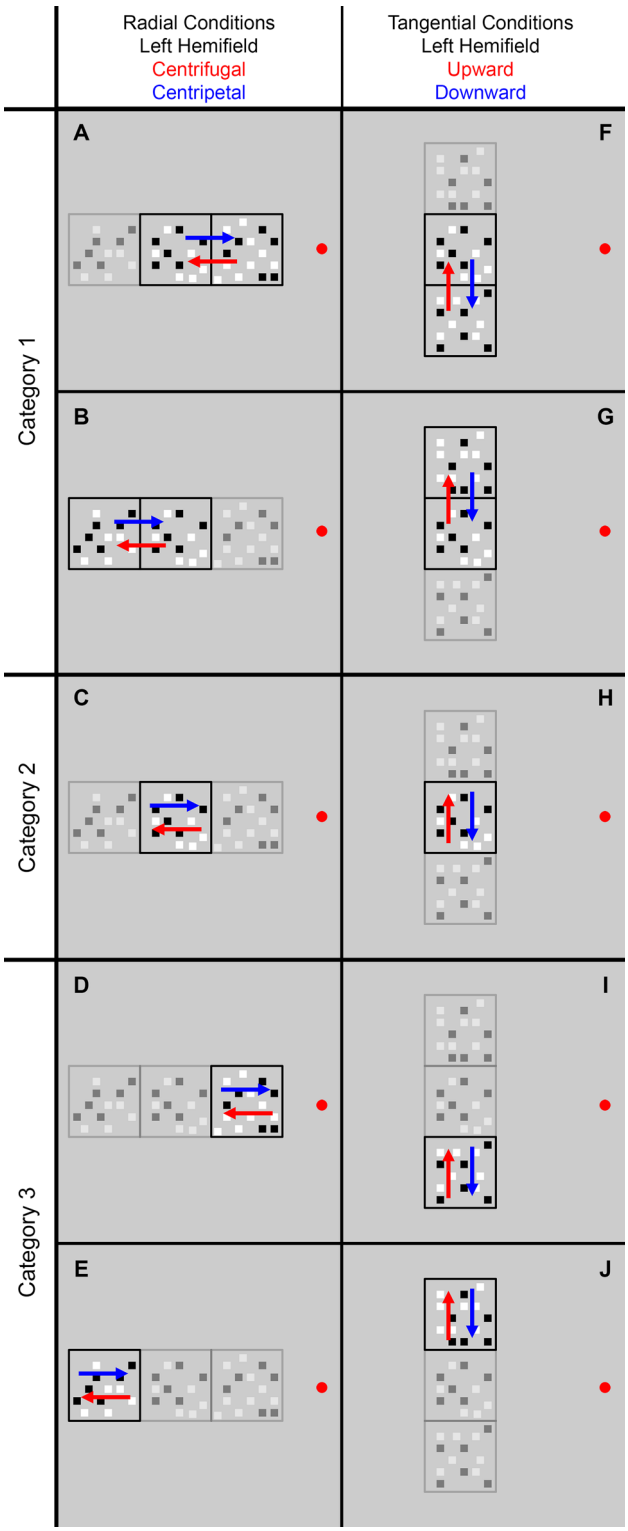

◀**Fig. 2** Main experiment stimulus locations. The positions of the motion stimuli presented in the left hemifield are depicted for radial motion (**a**–**e**) and tangential motion (**f**–**j**). Motion was presented in the following motion areas: **a** target and central, **b** target and peripheral, **c** target, **d** central, **e** peripheral, **f** target and lower, **g** target and upper, **h** target, **i** lower and **j** upper. The *colored arrows* denote the different motion directions. At the areas, which are shown having lesser opacity in this schematic, *stationary dots* were shown during the MRI experiments. Presentation in the right hemifield (not depicted) was an exact mirror image of this schematic. Stimuli were presented simultaneously in both hemifields

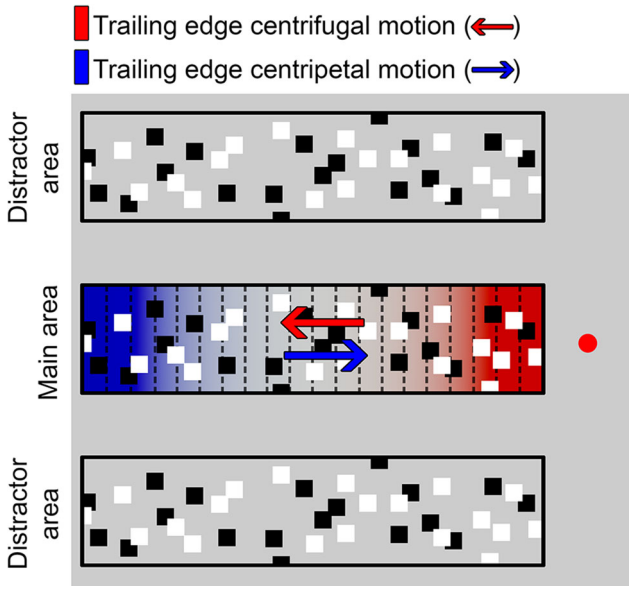

Fig. 3 Control experiment stimulus. The figure shows the motion stimuli presented in the left hemifield during the control experiment. BOLD responses were obtained from the *rectangular area* along the horizontal meridian (main area) at 20 equally spaced locations, denoted by *dashed lines*. *Dots* in this area moved either in centrifugal or centripetal directions (*arrows*). The location of the trailing edge depended on the motion direction, which is denoted by *colors* within the main area. The *colors* of the trailing edge locations are in correspondence with the *colored arrows* of the motion directions. Above and below, 2 additional stimuli were presented: the distractor areas. *Dots* in the distractor areas either moved in the opposite direction of the dots in the area at the main area, or remained stationary. Presentation in the right hemifield (not depicted) was an exact mirror image of this schematic. Stimuli were presented simultaneously in both hemifields

Additionally, four rectangular areas of equal dimensions and similar dot distribution, the distractor areas, were positioned above and below the main area (Fig. 3). If new appearing dots draw spatial attention, causing elevated BOLD responses, the presentation of 3 times more novel dots would reduce the signal at all trailing edges in equal proportions. This would not happen, if elevated BOLD responses are the result of novel dots per se. To minimize direct influence of the distractor areas on the main area, there remained a blank space of 2.2° visual angle between motion areas. There were two conditions regarding the distractor areas: dots either moved in the opposite direction of the main area dots with equal velocity, or the distractor area dots remained stationary, while motion was shown over the main area. The full setup resulted in 4 conditions

(2 motion directions × 2 distractor area conditions), which was repeated 8 times (640 volumes).

Attention task

During all motion experiments (i.e. main and control experiments), a white cross was projected every 1,000 ms. During approximately 25 % of all cross-projections, an additional small triangle was presented, that transformed one of the bars of the white cross in an arrow pointing in one of four directions: left, right, up or down. The participants were instructed to respond with a button press that corresponded to the direction of the presented arrow, using a button box with four buttons. A correct response was counted, if participants pressed the correct corresponding button before the next attention cue was presented. If a non-corresponding button was pressed, the response was incorrect. When participants failed to press a button before the next attention cue, it counted as a missed response. The inter-trial interval and arrow direction were randomized.

Image analysis

All functional images were spatially preprocessed using SPM8 (http://www.fil.ion.ucl.ac.uk/spm/). The preprocessing entailed the realignment of all functional images to the mean image, slice time correction and co-registration to the anatomical image (T1). The T1 image was corrected for field inhomogeneities by dividing the T1 image by the proton density image (Van de Moortele et al. 2009).

Surface reconstructions for each hemisphere were created with the Computerized Anatomical Reconstruction and Editing Toolkit [CARET, (Van Essen et al. 2001)]. The reconstructed surfaces contained on average 1.6 nodes/mm^2. All functional images were mapped onto the surfaces of the left and right hemispheres, using a metric Gaussian mapping algorithm, resulting in a time series for every node of the surface. Low-frequency noise was removed using multiple regression and a design matrix containing the mean of each image and six cosine functions per experiment, which formed a high-pass filter with a cutoff at 3.3×10^{-2} Hz.

For the polar angle mapping stimulus, we used a phase-encoded regressor-matrix to obtain the polar angles for the nodes on the reconstructed cortical surface. The regressor matrix contained a regressor for every scan during a stimulus cycle and represented the cyclic activation of the rotating wedge (6,400 ms activation during every 48,000 ms cycle), which was convolved with a hemodynamic response function (Friston et al. 1995). A correlation coefficient was calculated for every regressor in the regressor matrix (i.e., every image in a cycle) for every node of the reconstructed surface. The peak correlation of a node determined the polar angle of a node's receptive field. The polar angle results were used to draw ROIs on the reconstructed surfaces of each hemisphere, and included the early visual cortical areas V1, V2, and V3.

Main experiment

The motion area mapping stimulus was analyzed with a multiple linear regression analysis, using a design matrix that contained five factors, one for each motion area. The analysis resulted in five *T*-statistics per node on the surface. Only nodes on the surface that responded to the target motion area ($T \geq 4.51$), and that were situated within V1, V2, or V3, were included. The *T*-statistics of the remaining 4 motion areas were used to exclude nodes that represented part of the target area, but whose activation could also be influenced by stimulation from adjacent squares. Nodes were excluded if the *T*-value for the factor corresponding to one of the adjacent areas exceeded 2.71. This procedure resulted in on average 104 included nodes (SD = 27) on the reconstructed surfaces of both hemispheres per subject. Thus, these nodes responded to the target motion area and not to any of the other motion areas.

For the radial and tangential motion experiments, we estimated the BOLD amplitude at the target motion area surface nodes, using a linear regression with a design matrix that contained factors for all stimulus conditions. To test for significant differences in the BOLD amplitude between stimulus conditions within the three categories, three GLM repeated measures designs were adopted. All GLMs included the three visual areas as independent measures and the radial/tangential groups as a between-subjects factor. The first GLM tested for differences in BOLD amplitude between leading or trailing edge bordering the target motion area. This GLM contained leading/trailing edge as within-subjects factor. The second GLM was designed to test for difference in the BOLD amplitude between radial and tangential motion directions (i.e., centrifugal/centripetal vs. upward/downward motion directions), when motion was presented solely over the target motion area. This GLM contained opposite motion directions (i.e., centrifugal/centripetal and upward/downward) as within-subjects factor. The third GLM again tested for differences between leading or trailing edges bordering the target motion area, while motion was presented outside the target motion area, and contained leading/trailing edge as within-subjects factor.

Control experiment

For the main area mapping stimulus, we used a phase-encoded regressor matrix to establish cortical representations of all 20 locations on the reconstructed cortical

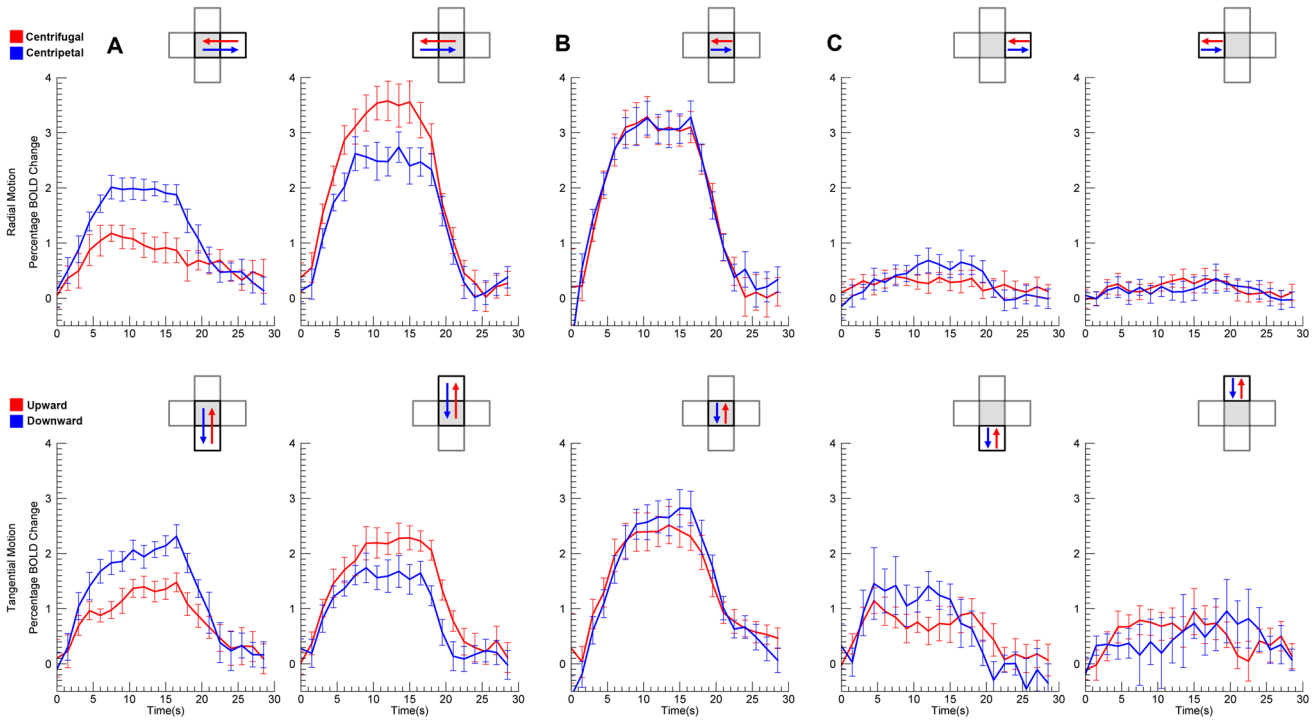

Fig. 4 Signal change main experiment. Figures show the BOLD signal change (mean V1, V2, V3) for radial (*upper row*) and tangential (*lower row*) motion directions. A schematic of the stimulus conditions (left hemifield) is shown in the *top right corner* of each individual plot (target motion area in *gray*). *Colored arrows* in the schematic correspond with the colors of the BOLD response. **a** Motion is presented at the target motion area and 1 adjacent motion area. For motion presented in any 2 motion areas, the motion direction determined the distance of the target motion area to the leading and trailing edges. **b** Motion is presented at the target motion area only. Relative to the target motion area, there is no difference in the distance to leading or trailing edges. **c** Motion is presented only in 1 motion area adjacent to the target motion area. Neither the leading nor trailing edge was directly present over the target motion area. *Error bars* denote standard error of the mean across subjects

surface. The regressor matrix contained 20 regressors, 1 for each location, and represented the cyclic activation of each node (7,300 ms activation during every 30,000 ms), which was convolved with a hemodynamic response function (Friston et al. 1995). A correlation coefficient was calculated for every regressor in the regressor matrix, and the peak correlation determined to which of the 20 locations a node was most responsive. Additionally, *T*-statistics were calculated for every peak correlation, and only those nodes were included that showed a *T*-value of $T \geq 4.51$, and that were situated in V1, V2, or V3.

We estimated the BOLD amplitude at all 20 locations using a linear regression with a design matrix that contained factors that represented the BOLD activation for all 4 motion conditions of the control experiment. To test for significant effects of the motion direction, we performed a paired sample *T* test per location of the main area (centrifugal vs centripetal). To test for significant effects between distractor areas with moving and stationary dots on the main area representations, a multivariate repeated measures design was used. The three visual areas were included as independent measures and distractor square condition as within-subject factor.

Results

We presented various visual motion stimuli in 25 healthy subjects, while measuring brain activation with fMRI. The main experiment ($n = 16$) was designed to test the effect of predictable contrast changes at a motion stimuli's leading edge versus unpredictable contrast changes at a motion stimuli's trailing edge on the amplitude of the BOLD signal. We did this by showing moving dots in five predefined motion areas in each hemifield, while we measured the BOLD response in the target motion area only. Using three categories of motion stimuli, we varied the distance of leading and trailing edges relative to the target motion area. This setup allowed us to assess the effect of leading and trailing motion edges in the exact same retinotopic area (i.e., target motion area) for the different stimulus configurations.

To measure the effect of distance towards the motion stimuli's leading and trailing edges on the BOLD signal, motion was presented in two adjacent motion areas (Fig. 2: Category 1). The motion direction determined whether the leading or trailing edge bordered the target motion area. We found that the motion direction had a large effect on

the BOLD amplitude ($F_{(3,12)} = 15.967$, $p < 0.001$), while motion was present over the target motion area; a short distance between the leading edge and target motion area resulted in lower BOLD amplitudes, compared to a short distance between motion target area and the trailing edge (Fig. 4a). In addition, there was no significant difference between radial and tangential motion directions ($F_{(3,12)} = 1.000$, $p = 0.426$). Thus, these results indicate that BOLD amplitudes to a moving random dot pattern depend on the distance of the motion stimulus' leading or trailing edge to the target motion area. When the trailing edge was near the target motion area, amplitudes of the BOLD signal were higher than when the leading edge was near the target motion area (Fig. 5). These results are true for both radial and tangential motion directions, showing the possible presence of predictive coding effects in early visual areas.

To assess whether activity in the target motion area could have been biased by local anisotropies towards particular motion directions, we measured BOLD amplitudes when the stimuli's leading *and* trailing edges were both bordering the target motion area (Fig. 2: Category 2). Therefore, changing the motion direction had no effect on distances towards leading and trailing edges relative to target motion area. Subsequently, we found no effect of motion directions for radial ($F_{(3,5)} = 0.053$, $p = 0.982$) and tangential ($F_{(3,5)} = 2.396$, $p = 0.184$) directions (Fig. 4b), nor did we find a general difference between radial and tangential directions ($F_{(3,12)} = 0.782$, $p = 0.526$). These results exclude the possibility that local anisotropies for different motion directions can explain our findings.

In addition, to check if effects of leading and trailing motion edges were caused by motion-induced shifts in the cortical location of the stimulus representation, as has been suggested by previous research (Whitney et al. 2003), we measured activation for the target motion area, while motion was only presented in an adjacent area (Fig. 2: Category 3). Putative effects of a motion-induced flexible retinotopy should be evident under this stimulus configuration. To the contrary, we found no significant effect of motion direction on the BOLD amplitude in the target motion area representation ($F_{(3,12)} = 2.546$, $p = 0.105$). Therefore, it is unlikely that motion-induced shifts in the location of the stimulus representation can account for differences between leading and trailing motion edges (Fig. 4c).

The control stimulus was designed to measure the maximum extent of biased BOLD responses near the trailing edge, to assess the possible contribution of extra-classical receptive field effects. We found that the biases were not merely restricted to the edge representations. Para-foveally, biases stretched from 1° to approximately 3° visual angle, and peripherally, biases were measured from approximately 14° to 10° visual angle (Fig. 6). Biased

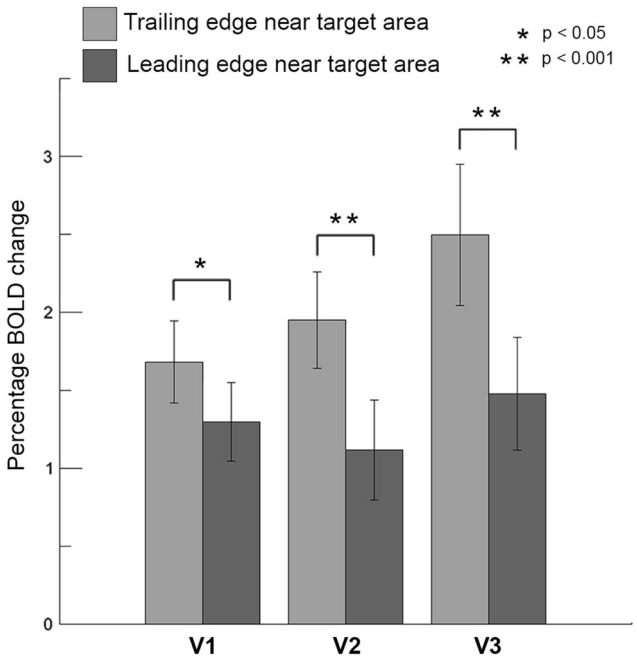

Fig. 5 BOLD amplitudes trailing and leading edges. The estimated peak signal change is shown for Category A stimuli during the main experiment (both radial and tangential). Stimulus conditions that presented the trailing motion edge bordering the target motion area are shown by the *light gray bars*, while stimulus conditions that presented the leading motion edge bordering the target motion area are shown by the *dark gray bars*. From *left* to *right* the amplitude at separate visual areas is shown. *Error bars* denote standard error of the mean across subjects and the *asterisks* indicate significant levels

responses were also clearly visible on the level of individual subjects (Fig. 7). The range in which enlarged BOLD responses were present is well beyond the sizes of classical (population) receptive fields to be found in early visual cortex, indicating that extraclassical receptive effects must have contributed to observed effects (Dumoulin and Wandell 2008).

Lastly, the BOLD activity difference between leading and trailing edge can be explained by (covert) visuo-spatial attention shifts towards novel dots at the trailing edge. To estimate the possible contribution of attention shifts, distractor dot patterns were presented during the control stimulus (Fig. 3). The distractor dot patterns either moved in opposite direction of the main area dot pattern, or did not move at all. Moving distractor dot patterns presented subjects with a threefold increase in leading and trailing edges, compared to the stationary distractor condition. If spatial attention shifts are the cause of elevated BOLD responses near the trailing edge, this threefold increase would reduce the effect with roughly 66 % due to a division of attentional resources. However, whether distractor dots were moving or remained stationary had no effect on the BOLD signal ($F_{(3,6)} = 1.830$, $p = 0.242$). Moreover, during all experiments subjects were engaged in a demanding attention task at

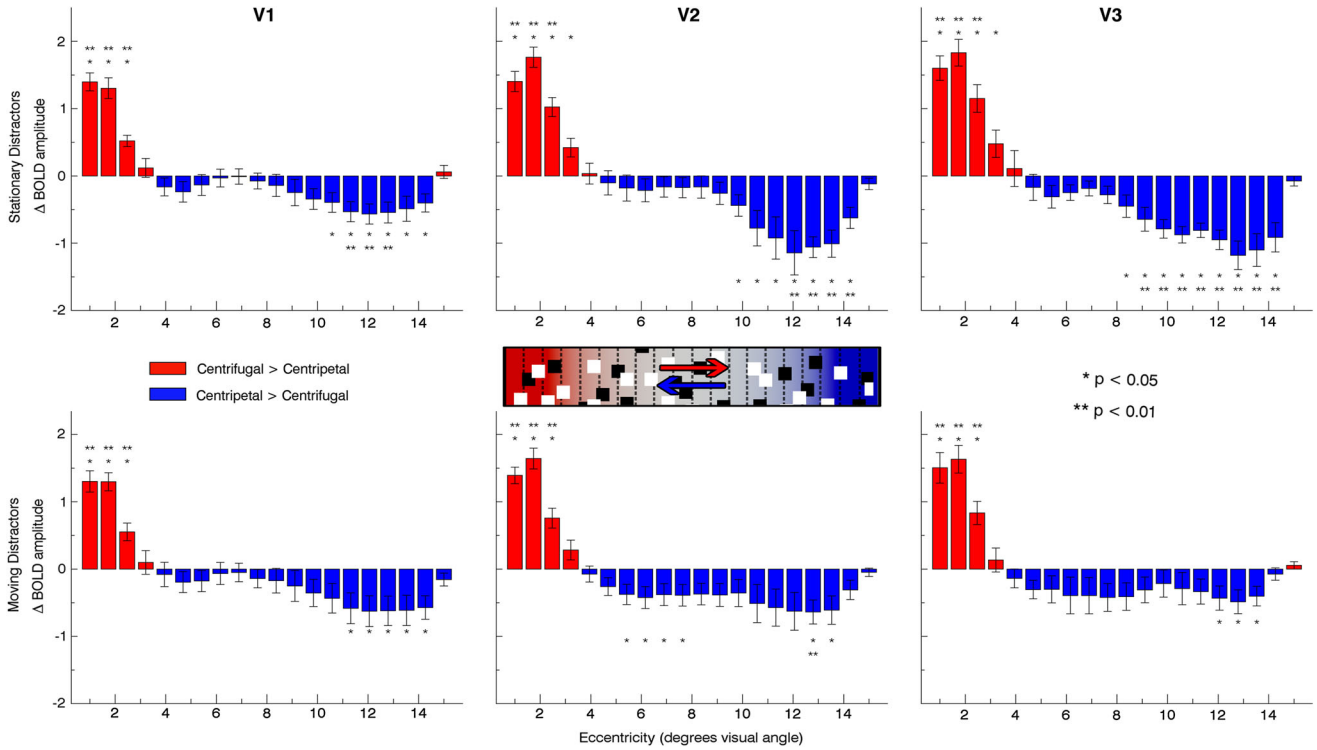

Fig. 6 Difference BOLD amplitude control experiment. Difference in estimated amplitudes of the BOLD signal during the control experiment between centrifugal and centripetal motion direction is shown for each location of the main area. *Red bars* signify locations where centrifugal motion resulted in larger signal changes compared to centripetal motion, and vice versa for the *blue bars*. Therefore, the amplitude of the bars approximate the effect size of the biased responses. The stimulus schematic of the control experiment is shown in the *center* of the figure. The *colored locations* within the center schematic (gradient) depict the trailing edge locations of each motion direction and correspond to the edge representations of the bar plots. *Graphs* from *left* to *right* show responses from separate visual areas. The *upper graphs* show responses when distractor area *dots* were stationary. The *lower graphs* show responses, when distractor area *dots* were moving. *Error bars* denote standard error of the mean across subjects

central fixation on which they had good but not perfect performance (86 % correct detections), making it exceedingly unlikely that effects of visuo-spatial attention can account for the observed effects.

Thus, the current results show that BOLD responses are relatively enlarged for unpreceded contrast changes at a motion stimulus' trailing edge compared to predictable contrast changes at the leading edge. Furthermore, we have been able to demonstrate that these effects are neither caused by differences in sensitivity to any presented motion direction (radial or tangential), nor by motion-induced shifts of cortical representations of the stimuli, nor by (covert) shifts in visuo-spatial attention to leading or trailing motion edges. Furthermore, we were able to show that enhanced activity for novel dots near the trailing edge most likely represent an extraclassical receptive field effect.

Discussion

In the current study, we hypothesize that neural activity in early visual cortex during perception of moving random stimuli depends on novelty, and therefore predictability, of visual input. Based on predictive coding, we expect increased BOLD signals for unpreceded contrast changes relative to contrast changes that have previously been detected by other neurons. In visual areas V1, V2, and V3, we indeed measured larger BOLD amplitudes near the trailing edge of a motion stimulus, where new dots enter the visual field, as opposed to smaller BOLD responses near the leading edge, where dots have traveled the maximum distance of the stimulus area. Furthermore, we excluded several alternative explanations for the observed findings, which indicate that some form of predictive coding for moving stimuli is present in early visual cortex.

We observed that cortical responses to motion decrease, when the trailing edge of a motion stimulus is distant from a retinotopic area, compared to the trailing edge being near that same retinotopic area. This phenomenon can also explain the directional motion biases we observed in the two previous studies (Raemaekers et al. 2009; Schellekens et al. 2013). These directional biases were observed for a large circular moving random dot stimulus (15° diameter) with an aperture at central fixation. Enhanced activation

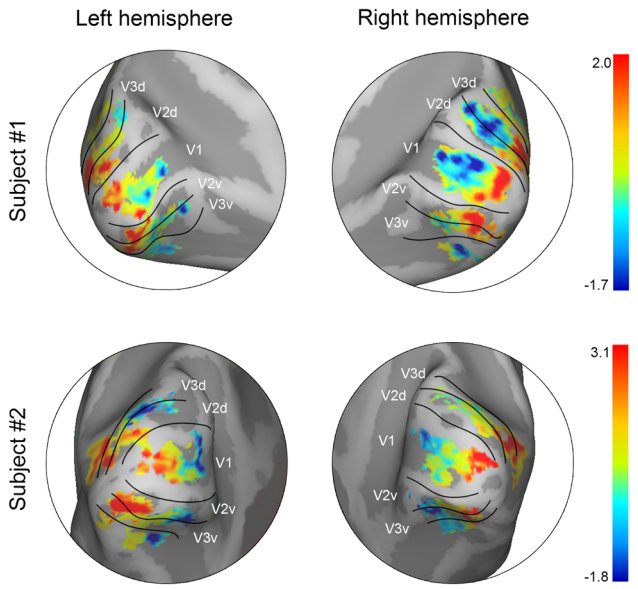

Fig. 7 Individual results control experiment. The difference between centrifugal and centripetal motion is shown on the inflated surface reconstructions (both hemispheres) of two subjects (*rows*), during the control experiment while distractor dots were stationary. The surface reconstructions show the medial-posterior view of the inflated occipital lobes. The foveal representation resides at the occipital pole. Cortical locations where centrifugal motion resulted in larger BOLD signal changes are depicted by *positive numbers* (i.e., parafoveal representations), while cortical locations where centripetal motion resulted in larger BOLD signal changes are depicted by *negative numbers* (i.e. peripheral representations). Borders between visual areas are denoted by the *black lines*. Note that BOLD activity is only present at cortical representations of the horizontal meridian (i.e. center V1 and border V2–V3), which represented the main area of the control stimulus. The cortical representation of the V1–V2 border corresponds to the vertical meridian, which was not subjected to any motion input

was found for centrifugal motion at low eccentricities, and for centripetal motion at high eccentricities. Probably, the centripetal bias at high eccentricity may be the result of novel dots entering the stimulus area at the trailing edge near the stimulus' outer rim, whereas the centrifugal bias at low eccentricity may be the result of a second trailing edge caused by the fixation aperture. Moreover, we have found that there exists no fundamental difference between radial and tangential motion directions. This contradicts the idea that directional motion biases share a common cause with the radial orientation bias (Sasaki et al. 2006; Clifford et al. 2009). In addition, it has been suggested that orientation selective cells in visual cortex are activated by motion streaks (Geisler 1999; Apthorp et al. 2009). Possibly, motion streaks cause different activation levels along a motion trajectory. However, under current experimental paradigms motion streaks would be roughly equal along the full motion trajectory. Hence, differences in motion streaks do not offer a plausible explanation for enhanced BOLD signals at the trailing edge, nor the gradual decrease in activity towards the leading edge, nor do different orientations of motion streaks exert a differential effect on BOLD responses to a moving random dot pattern. Instead, it is the novelty of moving visual input that explains different activation levels. Similar findings have been reported with different types of stimuli (Alink et al. 2010; Maloney et al. 2014), confirming that the amplitude of the BOLD response to motion stimuli depends on stimulus novelty or predictability.

The novelty of dots could additionally influence current observations in more than one way. At the trailing edge of a motion stimulus, moving dots enter the visual field from behind the stimulus aperture. This might cause moving dots to visually appear in the middle of a neuron's receptive field. Subsequently, this might cause a differential effect with respect to neurons signaling information at the leading edge, where moving dots drift into a neuron's receptive field (Borg-Graham et al. 1998; Gieselmann and Thiele 2008). Thus, the results could be due to classical receptive field effects, instead of stimulus predictability. However in the main experiment, we excluded the voxels that responded to motion areas directly adjacent to the target motion area. This automatically excludes voxels that were responsive to the edges of the target motion area, where new dots entered the visual field. As the size of the target motion area (4° × 4° visual angle at 7° eccentricity) by far exceeds receptive field sizes in V1, V2 and V3 (Dumoulin and Wandell 2008), there is a substantial number of voxels that responds solely to the stimulus' inner part. Although it is possible that some voxels included neurons that still responded to the edge of the target motion area, it is unlikely that they could have caused the large observed effects, as their relative contribution to the signal would simply be too small. Furthermore, when motion was presented outside, but directly adjacent to the target motion area, no significant differences in BOLD signal were detected. If only those voxels that represented the edge of the stimulus were causing the effect, the effect should also be pronounced during this condition. Finally, the control experiment showed that elevated BOLD responses were present beyond the range of classical receptive fields that represented the control stimulus' trailing edge. Hence, it is unlikely that the current results can be explained by differentiating classical receptive field effects for dots appearing in the center of receptive fields and dots drifting into receptive fields.

The difference in BOLD signal between predictable and unpreceded moving dots appears to be caused by extra-classical receptive field effects of local neuronal populations. This may also include (covert) visuo-spatial attention, which could shift to the stimulus part where novel dots appear. However, there are several reasons why spatial attention is an unsatisfactory explanation. First, the

effect was observed during stimulus presentation in two hemifields simultaneously. Although it has been shown that spatial attention can be divided over multiple visual field locations (Adamo et al. 2008), this certainly adds a restraint on its possible contribution. Secondly, the current study included an attention task at the location of the fixation dot. Performance on the attention task indicated that participants were able to maintain spatial attention directed at the center of the screen. Finally, the control experiment showed that the presentation of four additional motion stimuli had no effect on elevated BOLD responses near the trailing edge. If visuo-spatial attention was to cause elevated BOLD responses, dividing one's attention over four additional stimuli should have diminished the anticipated effect.

Predictive coding offers a plausible explanation for the observed effects, stating that unpreceded motion contrast changes at the trailing edge would yield larger prediction errors compared to predictable contrast changes near the leading edge. However, underlying mechanisms for predictive coding are still under debate. Currently, most predictive coding models incorporate predictive states, i.e., predictions for observational or otherwise lower-level input (Mumford 1992; Spratling 2008). Predictive states have among others been proposed as a construct of Bayesian inference (Lee and Mumford 2003) or a competition of many possible predictions (Spratling 2010). Additionally, extra-striate areas may accommodate predictive states for the primary visual cortex (Rao and Ballard 1999). Although we have found that motion novelty effects were largest in V3 (Fig. 4), the temporal limitations of fMRI BOLD do not allow us to infer that extra-striate areas hold predictions for area V1. However, predictive coding in early visual cortex would arguably be more efficient without actual predictions, for they might be computationally taxing for the visual system. If predictions are estimated for all neuronal input, predictive states virtually act as a buffer. Especially in early visual cortex, where receptive field sizes are small, it might be more expensive than beneficial to buffer the entire cortical visual field representation. Computational load further increases, as some models include an additional layer of prediction errors (Egner et al. 2010; Arnal et al. 2011).

Alternatively to predictive states, predictive coding may utilize simple heuristic mechanisms that have predictive outcomes. We propose a simplistic heuristic for motion processing, where detector activity in early visual cortex is suppressed from trailing to leading edge of the motion stimulus by means of corticocortical connections (Lamme et al. 1998; Angelucci et al. 2002). Automatic suppression along the motion direction would be computationally less demanding, since it would not need actual predictions and would also support preservation of energy resources (Friston 2010). Predictive coding without actual predictions has been previously suggested, where detector input is auto-correlated with input from neighboring detectors (Srinivasan et al. 1982). Such auto-correlation does not need actual predictions to be estimated. Similarly, a heuristic suppression mechanism for motion processing would affect neighboring motion and/or contrast detectors. A simple suppression mechanism is also supported by current results, when moving dots were presented outside the area of measurement, but moved towards the area of measurement. During this condition, a predictive mechanism based on predictive states would detect an unpreceded contrast change of opposite polarity, due to the fact that motion suddenly seizes to exist. However, this condition did not result in enhanced BOLD activity, which indicates that the mechanism underlying the observed effects is not based on predictive states. Our previous findings also support evidence for a suppression mechanism, showing motion biases when dots were randomly repositioned every 500 ms (Schellekens et al. 2013). Under such circumstances, predictions would match detector input to a lesser extent. However, we observed that random repositioning of dots did not attenuate motion biases, indicating that the effects observed during the current study are not based on matching input with predictions. Nonetheless, future studies are needed to resolve the actual processes of predictive coding for moving stimuli in early visual cortex.

Based on current results, no direct inferences can be made on the psychophysical correlates of the suppression effect on visual motion perception. However, recent studies have reported differences in detection thresholds of Gabor patterns that depended on the patterns' position and phase relative to a motion stimulus (Arnold et al. 2007; Roach et al. 2011). Both studies reveal lower detection thresholds for Gabor patterns that are located near the leading edge of a motion stimulus. In one study (Arnold et al. 2007), the authors argue that the discrepancy in Gabor pattern detection threshold is caused by flexible retinotopy (Whitney et al. 2003). However, we have been able to demonstrate that there are no novelty effects for motion stimuli presented directly adjacent to the area from where BOLD responses were obtained. This implies that flexible retinotopy, where motion induces shifts in cortical representation of the stimuli, cannot explain the observed findings. Alternatively, motion deblurring (or motion streak suppression) has been suggested to specifically target the motion trailing edge. (Marinovic and Arnold 2013; Arnold et al. 2014). If motion deblurring is underlying the current findings, then the enhanced BOLD activity near the trailing edge may in fact reflect increased inhibitory synaptic activity (Logothetis 2008). However, contribution of inhibitory processes to positive BOLD signal change is thought to be limited (Waldvogel et al. 2000; Goense and

Logothetis 2008), which makes a relative inhibition increase near the trailing edge seem at odds with current results. Instead, less excitatory activity offers a more straightforward interpretation of the reported signal decrease from trailing to leading edge, which is plausibly caused by a motion-induced predictive suppression mechanism. This may, in turn, have the previously reported psychophysical result of lower detection thresholds near a motion stimulus' leading edge due to a relative increase in available resources. Still, it is possible that the BOLD signal is comprised of additional mechanisms that specifically target motion trailing and leading edges (e.g., motion streak suppression).

To obtain further information on the currently observed motion-induced suppression, future studies should address motion displacement through motion velocity and motion duration. Arguably, these variables have large effects on the extent and range of the suppression. In addition, more data are needed to assess whether motion-induced suppression effects are related to certain perceptual qualities, such as motion direction discrimination (Lam et al. 2000; Webb et al. 2010) or motion saliency (Kastner et al. 1997). Finally, it would be interesting to see if predictive coding affects motion responses not only across visual space, but also in the spatiotemporal domain (Maus et al. 2013).

In conclusion, we found evidence for a predictive coding mechanism for motion processing in early visual cortex. The current results show that the near presence of a leading or trailing edge greatly determines the BOLD amplitude during observation of motion stimuli. Moreover, BOLD responses in early visual cortex directly reflect the predictability of motion information. The observed mechanism offers a more general and simpler explanation for motion biases, than differences in sensitivity for particular motion directions. These results could, thus, underlie the formation of stable percepts from an ever-changing scenery.

Acknowledgments This work was supported by a grant from the Dutch Organization for Scientific Research (NWO VENI 863.09.008).

References

Adamo M, Pun C, Pratt J, Ferber S (2008) Your divided attention, please! The maintenance of multiple attentional control sets over distinct regions in space. Cognition 107:295–303. doi:10.1016/j.cognition.2007.07.003

Alink A, Schwiedrzik CM, Kohler A et al (2010) Stimulus predictability reduces responses in primary visual cortex. J Neurosci 30:2960–2966. doi:10.1523/JNEUROSCI.3730-10.2010

Angelucci A, Levitt JB, Walton EJS et al (2002) Circuits for local and global signal integration in primary visual cortex. J Neurosci 22:8633–8646

Apthorp D, Wenderoth P, Alais D (2009) Motion streaks in fast motion rivalry cause orientation-selective suppression. J Vis 9(5):1–14. doi:10.1167/9.5.10.Introduction

Arnal LH, Wyart V, Giraud A-L (2011) Transitions in neural oscillations reflect prediction errors generated in audiovisual speech. Nat Neurosci 14:797–801. doi:10.1038/nn.2810

Arnold DH, Thompson M, Johnston A (2007) Motion and position coding. Vision Res 47:2403–2410. doi:10.1016/j.visres.2007.04.025

Arnold DH, Marinovic W, Whitney D (2014) Visual motion modulates pattern sensitivity ahead, behind, and beside motion. Vision Res 98:99–106. doi:10.1016/j.visres.2014.03.003

Borg-Graham LJ, Monier C, Frégnac Y (1998) Visual input evokes transient and strong shunting inhibition in visual cortical neurons. Nature 393:369–373. doi:10.1038/30735

Clifford CWG, Mannion DJ, McDonald JS (2009) Radial biases in the processing of motion and motion-defined contours by human visual cortex. J Neurophysiol 102:2974–2981. doi:10.1152/jn.00411.2009

Dumoulin SO, Wandell BA (2008) Population receptive field estimates in human visual cortex. Neuroimage 39:647–660. doi:10.1016/j.neuroimage.2007.09.034

Egner T, Monti JM, Summerfield C (2010) Expectation and surprise determine neural population responses in the ventral visual stream. J Neurosci 30:16601–16608. doi:10.1523/JNEUROSCI.2770-10.2010

Friston K (2005) A theory of cortical responses. Philos Trans R Soc Lond B Biol Sci 360:815–836. doi:10.1098/rstb.2005.1622

Friston K (2010) The free-energy principle: a unified brain theory? Nat Rev Neurosci 11:127–138. doi:10.1038/nrn2787

Friston KJ, Frith CD, Turner R, Frackowiak RS (1995) Characterizing evoked hemodynamics with MRI. Neuroimage 2:157–165. doi:10.1006/nimg.1995.1018

Geisler WS (1999) Motion streaks provide a spatial code for motion direction. Nature 400:65–69. doi:10.1038/21886

Gieselmann M, Thiele A (2008) Comparison of spatial integration and surround suppression characteristics in spiking activity and the local field potential in macaque V1. Eur J Neurosci 28:447–459. doi:10.1111/j.1460-9568.2008.06358.x

Goense JBM, Logothetis NK (2008) Neurophysiology of the BOLD fMRI signal in awake monkeys. Curr Biol 18:631–640. doi:10.1016/j.cub.2008.03.054

Kastner S, Nothdurft HC, Pigarev IN (1997) Neuronal correlates of pop-out in cat striate cortex. Vision Res 37:371–376

Lam K, Kaneoke Y, Gunji A et al (2000) Magnetic response of human extrastriate cortex in the detection of coherent and incoherent motion. Neuroscience 97:1–10

Lamme AF, Supèr H, Spekreijse H (1998) Feedforward, horizontal, and feedback processing in the visual cortex. Curr Opin Neurobiol 8:529–535

Lee TS, Mumford D (2003) Hierarchical Bayesian inference in the visual cortex. J Opt Soc Am A: 20:1434. doi:10.1364/JOSAA.20.001434

Logothetis NK (2008) What we can do and what we cannot do with fMRI. Nature 453:869–878. doi:10.1038/nature06976

Maloney RT, Watson TL, Clifford CWG (2014) Determinants of motion response anisotropies in human early visual cortex: the role of configuration and eccentricity. Neuroimage 100:564–579. doi:10.1016/j.neuroimage.2014.06.057

Marinovic W, Arnold DH (2013) An illusory distortion of moving form driven by motion deblurring. Vision Res 88:47–54. doi:10.1016/j.visres.2013.05.009

Maus GW, Fischer J, Whitney D (2013) Motion-dependent representation of space in area MT+. Neuron 78:554–562. doi:10.1016/j.neuron.2013.03.010

McKeefry DJ, Watson JD, Frackowiak RS et al (1997) The activity in human areas V1/V2, V3, and V5 during the perception of

coherent and incoherent motion. Neuroimage 5:1–12. doi:10.1006/nimg.1996.0246

Mumford D (1992) On the computational architecture of the neocortex. Biol Cybern 66:241–251

Raemaekers M, Lankheet MJM, Moorman S et al (2009) Directional anisotropy of motion responses in retinotopic cortex. Hum Brain Mapp 30:3970–3980. doi:10.1002/hbm.20822

Rao RP, Ballard DH (1999) Predictive coding in the visual cortex: a functional interpretation of some extra-classical receptive-field effects. Nat Neurosci 2:79–87. doi:10.1038/4580

Roach NW, McGraw PV, Johnston A (2011) Visual motion induces a forward prediction of spatial pattern. Curr Biol 21:740–745. doi:10.1016/j.cub.2011.03.031

Sasaki Y, Rajimehr R, Kim BW et al (2006) The radial bias: a different slant on visual orientation sensitivity in human and nonhuman primates. Neuron 51:661–670. doi:10.1016/j.neuron.2006.07.021

Schellekens W, Van Wezel RJ, Petridou N et al (2013) Integration of motion responses underlying directional motion anisotropy in human early visual cortical areas. PLoS One 8:e67468. doi:10.1371/journal.pone.0067468

Spratling MW (2008) Predictive coding as a model of biased competition in visual attention. Vision Res 48:1391–1408. doi:10.1016/j.visres.2008.03.009

Spratling MW (2010) Predictive coding as a model of response properties in cortical area V1. J Neurosci 30:3531–3543. doi:10.1523/JNEUROSCI.4911-09.2010

Srinivasan MV, Laughlin SB, Dubs A (1982) Predictive coding: a fresh view of inhibition in the retina. Proc R Soc B Biol Sci 216:427–459. doi:10.1098/rspb.1982.0085

Van de Moortele P-F, Auerbach EJ, Olman C et al (2009) T1 weighted brain images at 7 Tesla unbiased for proton density, T2* contrast and RF coil receive B1 sensitivity with simultaneous vessel visualization. Neuroimage 46:432–446. doi:10.1016/j.neuroimage.2009.02.009.T

Van Essen DC, Drury HA, Dickson J et al (2001) An integrated software suite for surface-based analyses of cerebral cortex. J Am Med Inform Assoc 8:443–459

Wacongne C, Changeux J-P, Dehaene S (2012) A neuronal model of predictive coding accounting for the mismatch negativity. J Neurosci 32:3665–3678. doi:10.1523/JNEUROSCI.5003-11.2012

Waldvogel D, Van Gelderen P, Muellbacher W et al (2000) The relative metabolic demand of inhibition and excitation. Lett Nat 406:995–998

Webb BS, Ledgeway T, McGraw PV (2010) Relating spatial and temporal orientation pooling to population decoding solutions in human vision. Vision Res 50:2274–2283. doi:10.1016/j.visres.2010.04.019

Whitney D, Goltz HC, Thomas CG et al (2003) Flexible retinotopy: motion-dependent position coding in the visual cortex. Science 302:878–881. doi:10.1126/science.1087839